Int. J. Nanosci. Nanotechnol., Vol. 20, No. 4, Dec. 2024, pp. 285-294
DOI: 10.22034/ijnn.2025.2041148.2568

Electrocatalyst For Solid Oxide Fuel Cells Operating at Intermediate Temperatures

Mazhyn K. Skakov[1], Sana K. Kabdrakhmanova[2*], Esbol Shaimardan[3], Kydyrmolla, Akatan[4], Almira M. Zhilkashinova[4], Madiyar M. Beisebekov[2,3], Kantay Nurgamit[4], Arman Zh. Miniyazov[5], Viktor V. Baklanov[5], Yerbolat T. Koyanbayev[5], Nuriya M. Mukhamedova[5], Gainiya K. Zhanbolatova[5]

[1]RSE National nuclear center of the Republic of Kazakhstan, Kurchatov, Kazakhstan
[2]Satbayev University, 22, Satbayev str., Almaty, Kazakhstan
[3]Scientific Center of Composite Materials, 79 Nurmakov str., Almaty, Kazakhstan
[4]S. Amanzholov East Kazakhstan University, 55, Kazakhstan str., Ust-Kamenogorsk, Kazakhstan
[5]Institute of atomic energy branch RSE NNC RK, Kurchatov, Kazakhstan

(*) Corresponding author: skabdrakhmanova@gmail.com
(Received: 14 September 2024 and Accepted: 24 November 2024)

Abstract

The present study aims to advance the existing body of research on electrode materials used in electrochemical applications, specifically sustainable energy devices, such as solid oxide fuel cells (SOFCs). Synthesis and characterization of the Ce~0.8~Cu~0.1~Co~0.1~MnO~3~ electrocatalyst was performed, followed by analysis of the electrochemical properties of this complex oxide system. The electrocatalyst offers high activity in oxygen reactions at intermediate temperatures, and is considered to be a promising candidate for SOFCs that operate in such a range, as it shows significant improvement in catalytic activity. The structural and morphological features of Ce0.8Cu0.1Co0.1MnO3 have been examined using X-ray diffraction, scanning electron microscopy with energy dispersive X-ray spectroscopy, transmission electron microscopy and TEM analysis showed that particle size ranged from 40 nm to 80 nm. Brunauer-Emmett-Teller analysis showed that the calculated surface area of Ce-CCM was 196.1 m2/g, EIS demonstrated that at a temperature of 600 degrees, the current density was 1.1 W/cm2. This is 1.2 times higher than that of existing cathode materials. Further, the oxidation states and surface composition of the Cu and Co incorporated into the CeMnO3 matrix were confirmed through XPS analysis. The results point to the potential of this material being used as an electrocatalyst for efficient oxygen reactions in various energy harvesting devices.

Keywords: *Solid oxide fuel cells (SOFCs), Ce-CCM (Ce~0.8~Cu~0.1~Co~0.1~MnO~3~), electrocatalyst, electrocatalytic.*

1. INRODUCTION

Recently, sustainable energy solutions have been a major focus in chemistry. Solid oxide fuel cells (SOFCs) have emerged as an important candidate in terms of efficiency and environmental friendliness [1]. Many technologies, inclusive of SOFCs, require advanced electrocatalysts for efficient and sustainable energy conversion [2]. The development of such electrocatalysts for enhanced oxygen reactions is a challenge for both researchers and manufacturers. Conventionally, SOFCs that operate at higher temperatures have increased effectiveness [3, 4]. One of the main issues now is connected with the development of SOFCs that can operate at lower temperatures, which has led to the creation of advanced electrocatalysts for oxygen reactions, especially at intermediate temperatures [5-7]. (Recently, composite ceramic materials based on rare earth elements have been widely used as electrode materials in SOFC systems [8-10]. Particularly, a catalyst based on yttria-stabilized zirconia (YSZ) and nickel is often used [11, 12]. However, under the influence

of small amounts of additives in the fuel, nickel is poisoned and its catalytic activity decreases rapidly [13].

The literature review shows that ceramic materials that combine rare earth elements and d-elements have good potential in solving this problem, as such materials have high electron conductivity and strong resistance to poisoning [14-17]. [18-20] Some studies have demonstrated that a Cu-Ce anode possesses excellent conductivity and remarkable resistance to damage, particularly within the tubular and planar cells. In such a setup, the copper primarily serves as the conduit for the current, while the cerium exhibits notable catalytic activity in oxidation reactions. Moreover, the Cu-Ce anode material has been investigated for its ability to withstand corrosion induced by sulfur and redox reactions [10, 14]. Therefore, incorporating copper, which boasts catalytic activity comparable to nickel, in the fabrication of cathode and anode materials has a beneficial impact on lowering the operating temperature of the electrode-membrane unit and extending the longevity of the catalytic system [11, 15].

Here, copper, cobalt and manganese mainly act as current collectors, while lanthanum and cerium have an active catalytic property in the oxidation reaction [21]. In addition, d-elements have been found to be resistant to corrosion that occurs during the oxidation reaction [22-24]. Therefore, the use of d-elements, with high catalytic activity and thermal stability, in electrode materials can have a positive economic effect, by allowing the operating temperature of the SOFC system to be lower, thus prolonging the activity of the catalytic system and reducing associated costs [25, 26].

In this study, the focus is on the synthesis and characterization of a novel material suitable for high activity in oxygen reactions at intermediate temperatures. By leveraging insights from previous research on complex oxide systems, the current team explore and elucidate upon the electrochemical performance of $Ce_{\sim 0.8\sim}Cu_{\sim 0.1\sim}Co_{\sim 0.1\sim}MnO_{\sim 3\sim}$ (Ce-CCM) and its potential in enhancing oxygen reaction kinetics in electrochemical devices. This work contributes to ongoing efforts to develop electrode materials for SOFCs and other energy conversion technologies, with the ultimate goal of achieving sustainable and efficient energy solutions.

2. MATERIALS AND METHODS

2.1. Chemicals and Materials

Cerium (III) nitrate hexahydrate ($Ce(NO_3)_3 \cdot 6H_2O$, 99.99%), copper (II) sulfate pentahydrate ($CuSO_4 \cdot 5H_2O$, 98.0%), cobalt (II) nitrate hexahydrate ($Co(NO_3)_2 \cdot 6H_2O$, 98.0%), and manganese (II) nitrate tetrahydrate ($Mn(NO_3)_2 \cdot 4H_2O$ 97.0%) were purchased from Sigma-Aldrich. The original $Ce(NO_3)_3.6H_2O$ was pre-dried for 2 hours at a temperature of 110±2°C in order to remove adsorbed water molecules and carbon dioxide. All other reagents were used without preliminary purification.

2.2. Synthesis of Complex Oxides

The Ce-CCM cathode material was prepared by coprecipitation method using sodium hydroxide. For this purpose, a 1 M solution of metal nitrates was dissolved in 500 ml of deionized water at room temperature. A saturated solution of sodium hydroxide (NaOH) with a volume of 100 ml was chosen as a precipitant. In order to form a homogeneous precipitate, the precipitant was added dropwise to the Ce-CCM solution, which was continuously stirred. The filtered precipitate was dried at a temperature of 100±2°C for 24 hours. The resulting sediment was ground and homogenized in a Pulverisette-6 ball mill (FRITSCH, Germany) at 300 rpm for 60 minutes. Calcination was carried out by heat treatment at 800±5°C to ensure the formation of a new phase structure of metal oxides. The final product was Ce-CCM.

2.3. X-ray Diffractometry

The crystal structures of the substances were analyzed using an X′PertPRO diffractometer (Malvern Panalytical Empyrean, Netherlands), with monochromatized copper (CuKα) radiation at a scan step of 0.02°, K-Alpha1 [Å] 0.1542. The measurement angle was 10-45°, the X-ray tube voltage was 45 kV, the current intensity was 30 mA, and the measurement time at each step was 0.5 s. An aluminium rectangular multi-purpose sample holder (PW1172/01) was used for measurements, which were done in reflection mode.

2.4. Scanning Electron Microscope

The morphologies and structures of the cathodic samples were examined using a Crossbeam 540 high-vacuum scanning electron microscope (Zeiss, Germany). The elemental composition was determined with an energy dispersive x-ray spectrometer (Thermo Fisher Scientific, USA).

2.5. TEM Analysis

Micrographs of the images were obtained using a JEM 1400 transmission electron microscope (JEOL, Japan), with a resolution of 0.38 nm, an accelerating voltage of 120 kV, and a high-resolution CCD Morada digital camera (Olympus, Japan). Before performing TEM, the samples were crushed in an agate mortar, then a suspension of alcohol solution was added, with the combined solution treated using ultrasonic dispersion at a frequency of 44 kHz on an UZDN-2T ultrasonic generator (Electron, Russia). Afterwards, fixation was done on a perforated carbon film deposited on a copper net, then drying was allowed before measurements were taken. By statistically calculating the particle sizes in the TEM images, the distribution and average particle sizes of the catalysts were determined.

2.6 Adsorption Porosimetry

The textural characteristics of the catalysts synthesized were determined using low-temperature nitrogen adsorption porosimetry on an Autosorb-1 surface area and pore size analyzer (Quantachrome Instruments, USA) and an ASAP-2020 adsorption analyzer (Micromeritics, USA). In order to determine the dependence of V on P at a constant temperature, preliminary vacuuming was done for 3 hours at a temperature of 200-220°C in order to degas the samples, and, following the experiments, mathematical processing of the data was performed using the Brunauer-Emmett-Teller (BET) method, the error in measurement of which (Δ) was ±2.8%.

2.7. XPS Analysis

XPS spectra were obtained using a NEXSA X-ray photoelectron spectrometer (Thermo Fisher Scientific, USA) with a transmission energy of 50 eV for a survey scan and 20 eV for an individual scan, with an operating power of 380 W. XPS positions were mapped using the carbon (1s) peak at 284.5 eV. Before actual analysis, samples were pretreated in a Model DZF-6210 preparation chamber (LabSol, China) maintained at 10-9 Torr vacuum.

2.8. Electrochemical Impedance Spectroscopy

Galvanostatic assessments were conducted at a fixed current density of 0.44 A/cm-2. Electrochemical impedance spectroscopy (EIS) was performed using a Model CS310M EIS potentiostat/galvanostat (Corrtest, China). The EIS measurements were performed under open-circuit conditions across a frequency spectrum spanning from 0.1 Hz to 5 kHz, utilizing a signal amplitude of 10 mV, and at temperatures of 500°C, 550°C and 600°C.

3. RESULTS AND DISCUSSION

3.1. XRD Analysis

Figure 1 shows the X-ray diffraction pattern of Ce-CCM. The well-defined sharp peaks indicate the highly crystalline nature of the sample. These peaks match well with the characteristic peaks of Ce-CCM. The synthesized sample appears to be highly pure, as there are no secondary phase peaks. The slight shift in peak positions observed in the sample could be due to the change in lattice parameters introduced by the incorporation of Cu and Co into the CeMnO3. The Miller indices are: (110), (-111), (211), (111), (-112), (-202), (112), (202), (-113), (022), (310), (311), and (004). The space group Im-3m has a cubic lattice, which is indicative of $Ce_{\sim 0.8\sim}Cu_{\sim 0.1\sim}Co_{\sim 0.1\sim}MnO_{\sim 3\sim}$.

In [27-28] studies, electrode compositions for SOFCs based on Cu-MnCo and Cu-Ce were synthesized. It was found that the phase structure of the obtained ceramic materials forms a multi-phase structure depending on the introduced d-elements. This, in turn, has been observed to increase catalytic activity. It can be concluded that obtaining similar results in this study has a positive effect on increasing catalytic activity in oxygen oxidation.

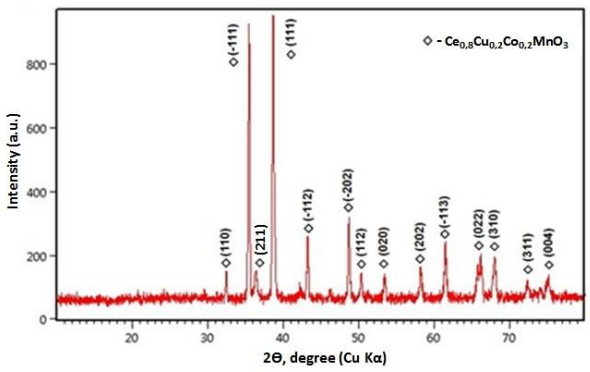

Figure 1. *X-ray diffractogram of Ce-CCM.*

3.2. SEM Analysis

SEM images of the Ce-CCM sample show the porous network of the microstructure to have a high surface area (Figure 2), which can enhance the diffusion of gases and is highly useful for electrocatalytic applications. The average pore diameter is in the range of 250 nm to 350 nm. The interconnected network of the material, with diameters in the range of 150 nm to 500 nm, helps to contribute to the mechanical stability of the material. Overall, the porous network microstructure evident from the SEM images can contribute to efficient oxygen ion and electron transport, particularly significant for cathode material applications in intermediate-temperature SOFCs.

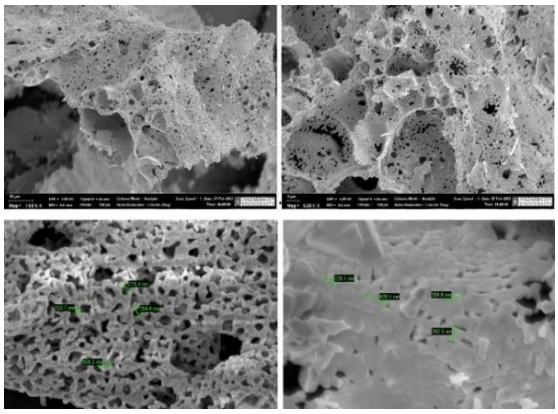

Figure 2. *SEM images of Ce-CCM.*

The energy dispersive X-RAY spectrum, coupled with SEM analysis, presents the detailed elemental composition of the Ce-CCM sample (Figure 3). The spectra clearly demonstrate the presence Ce, Cu, Co and Mn. This is consistent with the stoichiometry of the sample synthesized. The absence of any other elements clearly indicates the effectiveness of the doping process and the high purity of the Ce-CCM sample. Purity and homogeneity are crucial for reliable and uniform catalytic activity and electrical conductivity.

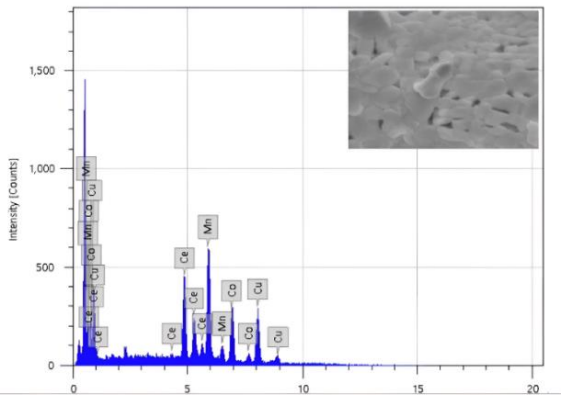

Figure 3. *Energy dispersive x-ray spectrum of Ce-CCM*

3.3. TEM Analysis

The microstructure and particle size details are evident in the TEM images of the Ce-CCM sample (Figure 4), which show that particle sizes range from approximately 40 nm to 80 nm. Such smaller-sized nanoparticles are likely to function as active catalyst sites, because the resultant higher surface areas could be beneficial for enhanced catalytic activity. In [29] the study the average particle size of the synthesized cathode material based on perovskite containing rare earth elements was found to be 100 nm. It was found that the smaller average particle size of the resulting cathode material improves the formation of a porous structure and increases the diffusion of oxygen on the catalyst surface. We see that the average particle size of the Ce-CCM synthesized in this study is approximately 1.25 times smaller than that determined in the [29] study.

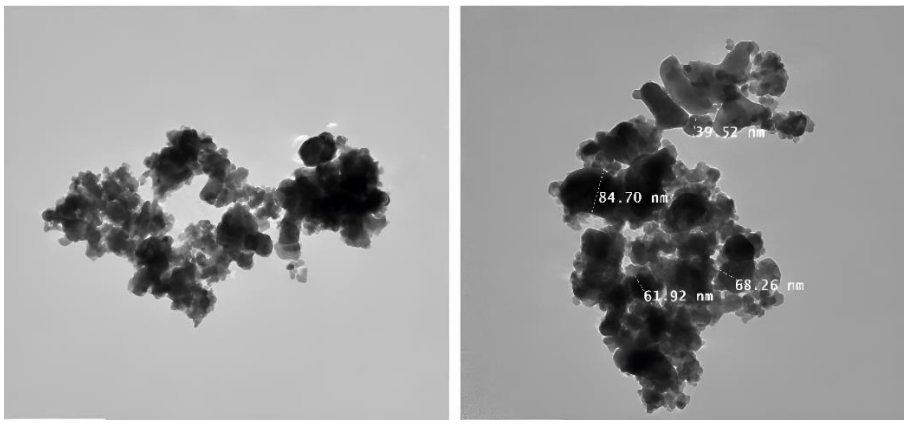

Figure 4. *TEM images of Ce-CCM.*

3.4. BET Analysis

The nitrogen adsorption-desorption isotherms of the Ce-CCM sample are shown in Figure 5a. The plot displays a hysteresis curve indicating that the mesoporous material has diameters of 2-50 nm. This feature is typical for type IV isotherms. The high surface area and enhanced gas diffusion of mesoporous materials are critical for better catalytic action. Ce-CCM is shown to exhibit H1-type hysteresis. Ce-CCM demonstrates monolayer adsorption on the walls of the mesopores at relative pressure (P/P0) ranging from 0 to 0.8 atmosphere. Further, the nitrogen adsorption-desorption isotherms were analyzed to determine pore size distribution (Figure 5b). The calculated surface area of Ce-CCM was 196.1 m^2/g, with an average pore radius of ≈ 1.38 nm, indicating a relatively moderate surface area, which is beneficial for catalytic surface reactions. The pore volume of 0.4 cm^3/g suggests the presence of micro- to mesopores within the sample. The half pore width measured from pore size distribution confirms the mesoporous range. The observed mesoporous structure in the synthesized material can facilitate enhanced oxygen ion transport and electrocatalytic performance. The authors of the study [30-32] obtained similar results when studying the catalytic activity of electrocatalytic systems. This indicates that the results of this study are consistent with other studies.

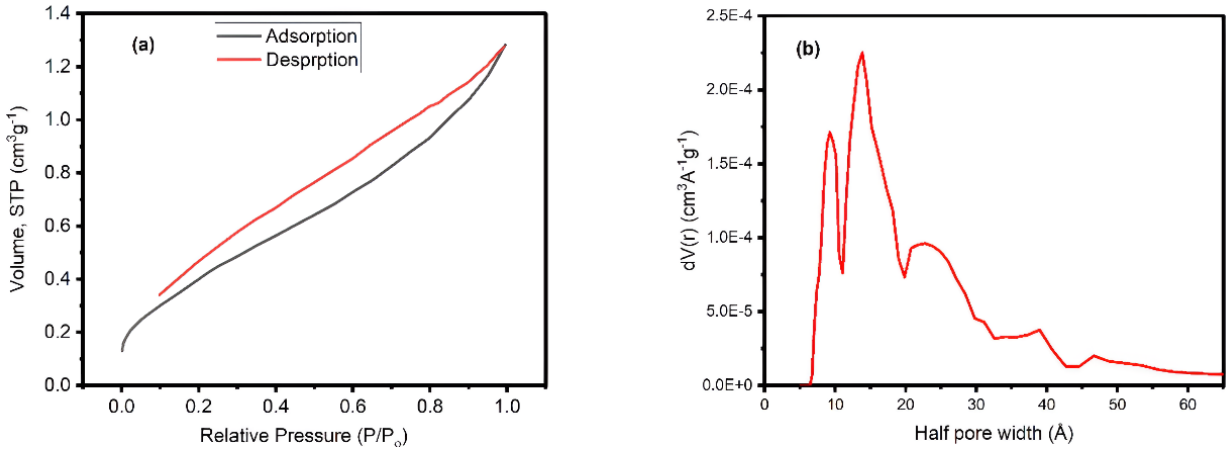

Figure 5. *Nitrogen adsorption-desorption isotherms of (a) Ce-CCM (b) Pore size distribution of Ce-CCM.*

3.5. XPS Analysis

The elemental composition and chemical states of the constituent elements were investigated through XPS analysis (Figure 6). In the Cu2p region, peaks are observed at 945 eV, 953 eV and 965 eV, which confirm the presence of Cu^{2+}. The peak at 953 eV corresponds to Cu 2p1/2. In the Co2p region, peaks are observed at 863 eV and 867 eV, which are characteristic of the Co^{2+} and Co^{3+} oxidation states. The 846 eV and 851 eV peaks in the Ce3d region show the 3d3/2 level, confirming the presence of the Ce^{3+} and Ce^{4+} oxidation states, while the Ce 3d5/2 level is indicated by the 863 eV and 867 eV peaks. These results confirm that Ce-CCM contains mixed valence states for Ce, Cu and Co, which are essential for high catalytic activity in oxygen reduction reactions. Studies [33-34] have shown that mixed oxides in different oxidation states can form highly active electrochemical centers and improve oxygen transport by optimizing its sorption. In addition, BET analysis revealed that mesoporousness positively affects the rapid diffusion of oxygen. The BET analysis results in this study (Figure 5) revealed that Ce-CCM is mesoporous.

3.6. Electrochemical Impedance Spectroscopy

The electrochemical study of the $Ce_{\sim 0.8\sim}Cu_{\sim 0.1\sim}Co_{\sim 0.1\sim}MnO_{\sim 3\sim}$ cathode material over a temperature range of 500-600 ºC is shown in Figure 7a. The peak power densities at 500, 550 and 600 ºC were found to be 0.41 W/cm^2, 0.58 W/cm2 and 1.1 W/cm^2, respectively. It was observed that power densities at 600 °C increased by up to 2.7 times compared to 500 °C. In this study [35] it was found that the cathode material based on $Ba_{0.5}Sr_{0.5}Co_{0.8}Fe_{0.2}O3_{-\delta}$ has a power density of 0.924 W/cm^2 at 700 °C. We see that the result obtained in this study is 1.2 times higher than the result determined in the [35] study. This indicates the potential for using Ce-CCM as a cathode material.

These responses, measured at relatively low temperatures, highlight the potential for use of this material in SOFC cathode applications. Nonetheless, more effective power generation capability is observed at higher temperatures. The temperature dependence of electrochemical impedance curves for at all three temperatures can be seen in Figure 7b. The high frequency intercept on the real axis is at the origin for all three temperatures, which clearly shows the minimal contact resistance, as indicated by ohmic resistance, and is consistent across all the temperatures. Semi-circular plots, resulting from the application of a simple Randles circuit, show that the diameter, indicating charge transfer resistance, decreases with temperature, thus Z^{l} is 1.35 (500 ºC), 0.6 (550 ºC) and 0.4

(600 ºC). Further, a significant reduction in charge transfer can be seen with the rise in temperature, where Z^{II} is 0.17 (500 ºC), 0.05 (550 ºC) and 0.025 (600 ºC). A similar trend of reduction is also seen with regards to peak imaginary impedance values when temperature is increased, indicating a decrease in the capacitive nature or the time constant of the charge transfer process. Practically speaking, as temperature increases charge transfer kinetics improve. Overall, at higher temperatures, the SOFC cathode material shows better performance, faster charge transfer, and lower resistive losses.

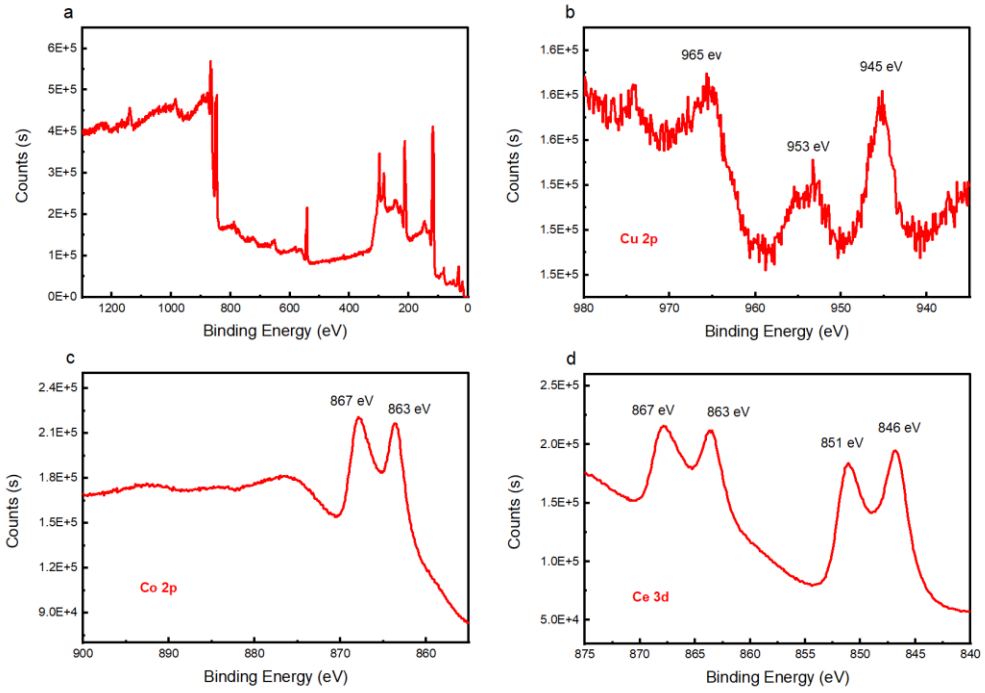

Figure 6. *XPS Photoelectron spectra of Ce-CCM.*

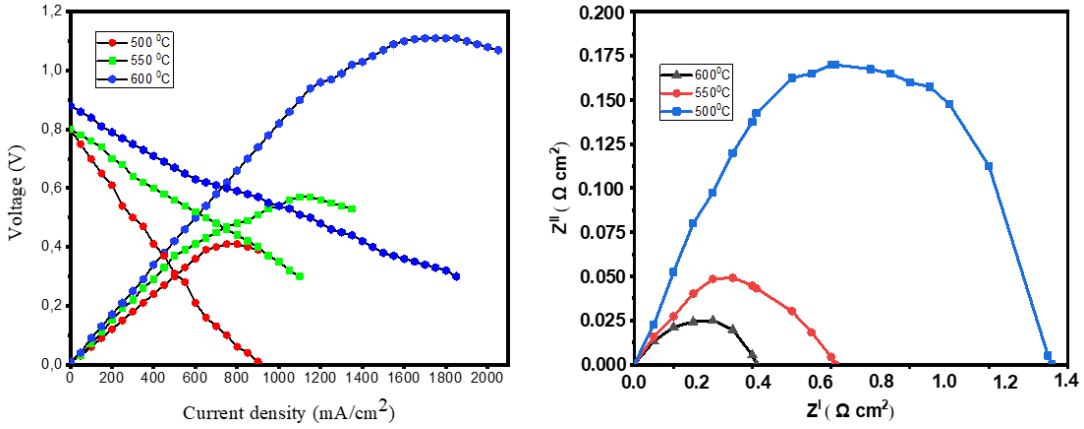

Figure 7. *Temperature and voltage (V) dependence on* ***(a)*** *current density (mA/cm^2) and* ***(b)*** *Temperature dependence on electrochemical impedance (Ω cm^2).*

4. CONCLUSIONS

In this study, a sample of Ce~0.8~Cu~0.1~Co~0.1~MnO~3~ (Ce-CCM) was synthesized by incorporating Cu and Co through the co-precipitation method, followed by characterization of its structural, morphological and electro-chemical properties. The crystallinity, phase purity and lattice parameters of the material change with the incorporation of Cu and Co, as confirmed by XRD. SEM analysis showed the network microstructure of the sample to be porous, while the coupled EDS measurements determined the elemental composition to be Ce, Cu, Co and Mn. TEM analysis revealed that particle size ranged from 40 nm to 80 nm. The mesoporous structure, with a half pore width mode of 13.845 Å, contributes to efficient gas diffusion and enhanced electrocatalytic performance, the calculated surface area of Ce-CCM was 196.1 m2/g, with an average pore radius of ≈ 1.38 nm, as investigated via BET analysis. EIS demonstrated that the performance of the material was quite good, it was found that at a temperature of 600 degrees, the current density was 1.1 W/cm2. This is 1.2 times higher than existing cathode materials, which is still much lower than that at which traditional solid oxide fuel cells (SOFCs) operate. Further, the oxidation states and surface composition of the Cu and Co incorporated into the CeMnO3 matrix were confirmed through XPS analysis, which indicates that the pure and porous crystalline networks of such Ce-CCM cathodes, with their favorable electrochemical properties, are promising for enhancing both the performance and efficiency of intermediate-temperature SOFCs. While the results of the current electrode material show promise, in the drive to reduce costs and improve efficiency in energy generation, additional formulations should be examined, with the goal of raising power output and lowering operating temperatures. We see that the Ce-CCM material has the potential to be used as a cathode for SOFCs and that further research is needed.

ACKNOWLEDGEMENT

This research has been funded by the Science Committee of the Ministry of Science and Higher Education of the Republic of Kazakhstan (Grant No. BR21882200).

CONFLICT OF INTEREST

The authors declare that they have no conflict of interest.

AUTHOR CONTRIBUTION

All authors contributed to the study conception and design.

REFERENCES

1. Singh, B., Ghosh, S., Aich, S., Roy, B., “Low temperature solid oxide electrolytes (LT-SOE) A review”, *J. Power Sources,* 339 (2017) 103-135.
2. Lee, S., Lee, K., Jang, Y. H., Bae, J., “Fabrication of solid oxide fuel cells (SOFCs) by solvent-controlled co-tape casting technique”, *Int. J. Hydrogen Energy*, 42 (2016) 1648-1660.
3. Fallah Vostakola, M., Amini Horri, B. “Progress in Material Development for Low-Temperature Solid Oxide Fuel Cells, A Review”. *Energies*, 14 (2021) 1280. https://doi.org/10.3390/en14051280
4. Jaiswal, N., Tanwar, K., Suman, R., Kumar, D., Uppadhya, S., Parkash, O. “A brief review on ceria based solid electrolytes for solid oxide fuel cells”, *J. Alloys Compd*, 781 (2019) 984-1005.
5. Da Silva, F.S., De Souza, T.M. ‘’Novel materials for solid oxide fuel cell technologies: A literature review’’ *Int. J. Hydrogen Energy*, 42 (2017) 26020-26036.
6. Patent for invention No. 36346, Skakov, M.K., Baklanov, V. V., Koyanbaev, E. T., Zhilkashinova, A. M., Kabdrakhmanova, S. K., Akatan, K., Shaimardan, E., Kantai, N., Pavlov, A.V., Miniyazov, A. Zh., Sokolov, I. A., Tulenbergenov, T. R., Kozhakhmetov E. A. “Sposob izgotovleniya tverdooksidnogo toplivnogo elementa” *applicant and patent holder RSE NNC RK*, 33 25.08.2023.
7. Fabbri, E., Pergolesi, D. Traversa, E. “Materials challenges toward proton-conducting oxide fuel cells: A critical review”, *Chem. Soc. Rev*, 39 (2010) 4355-4369.

8. Qiao, Z., Xia, C., Cai, Y., Afzal, M., Wang, H., Qiao, J., Zhu, B. "Electrochemical and electrical properties of doped CeO2-ZnO composite for low-temperature solid oxide fuel cell applications", *J. Power Sources*, 392 (2018) 33–40.
9. Zakaria, Z., Mat, Z. A., Hassan, S. H. A., Kar, Y. B. "A review of solid oxide fuel cell component fabrication methods toward lowering temperature", *Int. J. Energy Res*., 44 (2019) 594–611.
10. Wachsman, E. D., Lee, K. T., "Lowering the temperature of solid oxide fuel cells", *Science*, 334 (2011) 935–939.
11. Papurello, D., Lanzini, A., Fiorilli, S., Smeacetto, F., Singh, R., Santarelli, M. "Sulfur poisoning in Ni-anode solid oxide fuel cells (SOFCs): deactivation in single cells and a stack", *Chem. Eng. J.*, 283 (2016) 1224-1233. https://doi.org/10.1016/j.cej.2015.08.091
12. Al Kharusi, H., Svensson, M., Salamatinia, B., Horri, B. A. "Gelling synthesis of NiO/YSZ nanocomposite powder for solid oxide fuel cells", *Adv. Mater. Proc.*, 2 (2017) 813–818.
13. Choudhury, A., Chandra, H., Arora, A. "Application of solid oxide fuel cell technology for power generation—A review'', *Renew. Sustain. Energy Rev.*, 20 (2013) 430–442.
14. A. Esquirol, N. P., Brandon, J. A., Kilner, M., "Mogensen. Electrochemical Characterization of La0.6Sr0.4Co0.2Fe0.8O3 Cathodes for Intermediate-Temperature SOFCs", *Journal of The Electrochemical Society*, 151(11) (2004) 1847-1855.
15. Lee, K, Kang, J., Lee, J., Lee, S., Bae, J., "Evaluation of metal-supported solid oxide fuel cells (MS-SOFCs) fabricated at low temperature (1,000) using wet chemical coating processes and a catalyst wet impregnation method", *Int. J. Hydrogen Energy*, 43 (2018) 3786–3796.
16. K. Skakov, M., K. Kabdrakhmanova, S., Akatan, K., M. Zhilkashinova, A., Shaimardan, E., M. Beisebekov, M., Nurgamit, K., V. Baklanov, V., T. Koyanbayev, Y., Zh Miniyazov, A, A. Sokolov, I., and M. Mukhamedova, N., "La_2CuO_4 Electrode Material for Low Temperature Solid Oxide Fuel Cells", *ES Materials & Manufacturing*, 22 (2023) 969.
17. Bianco, M., Caliandro, P., Diethelm, S., Yang, S., Dellai, A., V. Herle, J., "In-situ experimental benchmarking of solid oxide fuel cell metal interconnect solutions", *Journal of Power Sources*, 461 (2020) 228163. https://doi.org/10.1016/j.jpowsour.2020.228163.
18. Marco, D. V., Grazioli, A., Sglavo, V. M., "Production of planar copper-based anode supported intermediate temperature solid oxide fuel cells cosintered at 950°C", *Journal of Power Sources*, 328 (2016) 235-240, doi: 10.1016/j.jpowsour.2016.08.025
19. Azzolini, A., Sglavo, V. M., Downs, J. A., "Production and performance of copper-based. Anode-supported SOFCs", *ECS Trans.*, 68 (2015) 2583-2596. doi: 10.1149/06801.2583ecst
20. Marco, V. D., Grazioli, A., Sglavo, V. M., "Production and Co-Sintering at 950°C of Planar Half Cells with CuO-GDC Cermet Supporting Anode and Li2O-Doped GDC Electrolyte", *Ceramic Engineering and Science Proceedings*, 37 (2016) 31-38. https://doi.org/10.1002/9781119320197.ch3
21. Kabdrakhmanova, S., Shaimardan, E., Akatan, K., Selenova, B., Zhilkashinova, A., Erbolatuly, D., Skakov, M., "Preparation and Characterization of the Catalyst Based on the Copper Nanoparticles", *International Journal of Nanoscience and Nanotechnology*, 18(1) (2022) 1-10.
22. Zurloa, F., Iannacib, A., M. Sglavob, V., Di-Bartolomeo, E. ''Copper-based electrodes for IT-SOFC'', *Journal of the European Ceramic Society,* 39 (2019) 17, https://doi.org/10.1016/j.jeurceramsoc.2018.02.029
23. De-Marco, V., Grazioli, A., Sglavo, V. M., "Production of planar copper-based anode supported intermediate temperature solid oxide fuel cells cosintered at 950 °C", *J Journal of Power Sources*, 328 (2016) 235240. doi: 10.1016/j.jpowsour.2016.08.025
24. Mesvari, S., Shariaty-Niassar, M., Karimi-Sabet, J., Dastbaz, A., "Lithium Extraction by Metal Organic Framework-Based Adsorbent (MnO2@Co/Zn ZIF) from Aqueous Solutions", *International Journal of Nanoscience and Nanotechnology*, 20(2) (2024) 129-142. 10.22034/ijnn.2024.2022011.2474
25. Dipti V. Dharmadhikari, Shrikant K. Nikam, Anjali A. Athawale, "Template free hydrothermal synthesis and gas sensing application of lanthanum cuprate (La2CuO4): Effect of precursors on phase formation and morphology", *Journal of Alloys and Compounds*, 590 (2014) 486-493.
26. Su, Y., Dai, L., Zhang, Q., "Fabrication of Cu-Doped CeO_2 Catalysts with Different Dimension Pore Structures for CO Catalytic Oxidation", *Catalysis Surveys from Asia*, 20 (2016) 231–240. https://doi.org/10.1007/s10563-016-9220-z
27. Li, S., Duan, Y., Zhou, Y., Yang, H., Zhang, Y., Wang, Q., Wang, J., Han, B., Zhu, L., Yang, J., Guan, W., Wu, A., "Research on the novel spinel structure of $Cu_{0.5}Ni_{0.5}MnCoO_4$ and its application in solid oxide fuel cells". *Ceramics International.*, 50(16) (2024) 27786-27795. https://doi.org/10.1016/j.ceramint.2024.05.076
28. Bochentyna, B. M., Chlipała, M. Gazda, Wang, S. F., Jasińsk,P., "Copper and cobalt co-doped ceria as an anode catalyst for DIR-SOFCs fueled by biogas", *Solid State Ionics*, 330 (2019) 47–53. https://doi.org/10.1016/j.ssi.2018.12.007
29. Choi, S., Yoo, S., Kim, J., "Highly efficient and robust cathode materials for low-temperature solid oxide fuel cells: PrBa0.5Sr0.5Co2−xFexO5+δ", *Sci Rep*, 3 (2013) 2426. https://doi.org/10.1038/srep02426

30. An, H., Park, W., Shin, H., Chung, D. Y., "Recommended practice for measurement and evaluation of oxygen evolution reaction electrocatalysis", *EcoMat.*, 6 (2024) e12486. https://doi.org/10.1002/eom2.12486
31. Razmara, Z., "Sonochemical synthesis, thermal behavior and luminescent properties of copper (II) supramolecular, a precursor for preparation of CuO nanoparticles and the study of their photocatalytic activity", *Journal of Inorganic and Organometallic Polymers and Materials*, 28 (2018) 2407-2417. doi: 10.1007/s10904-018-0906-8.
32. Golkhatmi, S. Z., Asghar, M. I., D. Lund, P., "A review on solid oxide fuel cell durability: Latest progress, mechanisms, and study tools", *Renewable and Sustainable Energy Reviews* 161 (2022) 112339, https://doi.org/10.1016/j.rser.2022.112339
33. Wolf, S., Roschger, M., Genorio, B., Garstenauer, D., Hacker, V., "Mixed Transition-Metal Oxides on Reduced Graphene Oxide as a Selective Catalyst for Alkaline Oxygen Reduction" *ACS Omega 8* (2023) 11536-11543. https://doi.org/10.1021/acsomega.3c00615
34. Gu, X. K., A. Camayang, J. C., Samira, S., Nikolla, E., "Oxygen evolution electrocatalysis using mixed metal oxides under acidic conditions: Challenges and opportunities", *Journal of Catalysis*, 388 (2020) 130-140. https://doi.org/10.1016/j.jcat.2020.05.008
35. Zhang, H., Chen, T., Huang, Z., Hu, G., Zhou, J., Wang, S., "A cathode-supported solid oxide fuel cell prepared by the phase-inversion tape casting and impregnating method*", International Journal of Hydrogen Energy*, 47(43) (2022) 18810-18819. https://doi.org/10.1016/j.ijhydene.2022.04.021